INVERSE PROBLEMS IN THEORY AND PRACTICE OF MEASUREMENTS AND METROLOGY

SEMENOV K. K., SOLOPCHENKO G. N.

Department of measurement informational technologies, St. Petersburg State Polytechnical University, 29, Polytechnicheskaya str., St. Petersburg, 195251, Russia

KREINOVICH V. YA.

Department of Computer Science, University of Texas at El Paso, 500 W. University, El Paso, TX 79968, USA

In this paper, we consider the role of inverse problems in metrology. We describe general methods of solving inverse problems which are useful in measurements practice. We also discuss how to modify these methods in situations in which there is a need for real-time data processing.

1. Introduction

What mathematical physics calls inverse problems is, in effect, the class of problems, which are fundamental in measurement theory and practice [1, 2]. The main objective of such problems is to develop procedures for acquiring information about objects and phenomena, accompanied by decreasing the distortion caused by the measuring instruments. Lord Rayleigh was the first to formulate such problem in 1871, on the example of spectroscopy. His purpose was to maximally decrease the influence of diffraction. Rayleigh showed that in mathematical terms, the problem of reconstructing the actual spectrum $x(\nu)$ from the measured signal $y(u)$ can be reformulated as the problem of solving an integral equation

$$y(u) = \int_{-\infty}^{\infty} K(u-\nu)\cdot x(\nu)\, d\nu \quad , \tag{1}$$

where $K(u-\nu)$ is the apparatus function of the spectrometer – which describes the distortion caused by diffraction.

The relation between inverse problems and measurements was emphasized by G. I. Vasilenko [3], who explicitly stated that the main objective of the inverse problem is "restoring the signals" or "reduction to the ideal instrument".

Eq. (1) is the integral Fredholm's equation of first type; it can be represented in the form $y(u) = \mathbf{A}\,x(v)$, where **A** is a compact linear operator of convolution – which describes a generic analog transformation of a signal inside a measuring instrument – and $K(u-\nu)$ is the kernel of this operator. From the mathematical viewpoint, the solution of Eq. (1) can be expressed as $x(v) = \mathbf{A}^{-1}\,y(u)$, where $\mathbf{A}^{-1}$ is the inverse operator to the compact operator **A**. From the practical viewpoint, however, we have a problem: it is known that such inverse operators are not bounded (see [4, p. 509]); as a result, a small noise in the measured signal can lead to drastic changes in the reconstructed solution $x(\nu)$. Such problems are known as ill-posed. A general approach of generating a physically reasonable solution to this problem – known as regularization – was formulated by A. N. Tikhonov in 1963 [5].

2. Inverse problems in metrology

If we take into account the inaccuracy $e(u)$ with which we register the output signal registration and the inaccuracy $\varepsilon(u-v)$ with which we know the apparatus function of the measurement device, then Eq. (1) will have the form $y(u) = \int_{-\infty}^{\infty} K_\varepsilon(u-\nu)x(\nu)d\nu + e(u)$. This equation with infinite (symmetric) integration limits describes spatial distortion processes in spectroscopy, chromatography, and in acoustic and other antenna-based measurements. For dynamic measurements – i.e., for measuring dynamic signals – the measurement result can only depend on the past values of the signal, so integration starts at 0:

$$y(t) = \int_0^{\infty} K_\varepsilon(t-\tau)x(\tau)d\tau + e(t) = \mathbf{A}_\varepsilon x(t) + e(t), \qquad (2)$$

where $\mathbf{A}_\varepsilon$ is the convolution operator with the kernel $K_\varepsilon(t-\tau)$ (known with inaccuracy $\varepsilon(t-\tau)$) and $e(t)$ is the additive noise.

The main idea behind Tikhonov's regularization is that we look for an (approximate) solution $\tilde{x}(t)$ to Eq. (2) by minimizing an appropriate stabilizing functional $\Omega(x(t))$ in Sobolev's space of smooth functions [5]. Usually, a functional $\Omega(x(t)) = \beta_0 \int_0^{\infty} \tilde{x}^2(t)dt + \beta_1 \int_0^{\infty} [\tilde{x}'(t)]^2 dt$, $\beta_0 > 0$ and $\beta_1 > 0$, is used on the

condition that the difference between $y(t)$ and $\mathbf{A}\,\tilde{x}(t)$ is of the same order as the error Δ caused by $e(t)$ and $\varepsilon(t)$: $\|\mathbf{A}\tilde{x}(t) - y(t)\|^2 = \Delta^2$. The Lagrange multiplier techniques reduces this constrained optimization problem to the unconstrained optimization of the functional [5]:

$$\min_{x(t)}\left[\|\mathbf{A}x(t) - y(t)\|^2 + \alpha\Omega(x(t))\right], \tag{3}$$

where α is called a regularization parameter.

2.1. *The minimal modulus principle*

When we have an *a priori* information about the norm of the solution and/or its derivative, we can find α. In particular, we can use fuzzy (imprecise) expert *a priori* information [6]. In the absence of such *a priori* information, we can use the principle of minimal modulus [7, 8] to select α.

This method is based on the fact that in the frequency domain, the stabilizing functional takes the form $\Omega(x(j\omega)) = \beta_0\int_0^\infty |x(j\omega)|^2 d\omega + \beta_1\int_0^\infty \omega^2 |x(j\omega)|^2 d\omega$, where j is imaginary unit and ω is circular frequency. The minimum of this functional is attained when the modulus $|x(j\omega)|$ is minimal.

Fourier transform of Eq. (2) leads to $y(j\omega) = K_\varepsilon(j\omega)\cdot x(j\omega) + e(j\omega)$. Based on 95% confidence intervals $K(\tau) - \varepsilon_{0.95}(\tau) \le K_\varepsilon(\tau) \le K(\tau) + \varepsilon_{0.95}(\tau)$ and $-e_{0.95}(t) \le e(t) \le e_{0.95}(t)$ in time domain, we can find the ellipses describing uncertainty in the frequency domain [9].

As a result, for every frequency ω_i we obtain two error-related ellipses in the complex plane: the first one centered in $y(j\omega_i)$ (Fourier transform of output signal) and another one centered at the value $K_\varepsilon(j\omega_i)$ (Fourier transform of apparatus function), as shown on Fig. 1. As shown in [7], for all values ω_i the value $\tilde{x}(j\omega_i)$ corresponding to the regularized solution is equal to $\tilde{x}(j\omega_i) = y_*(j\omega_i)/K^*(j\omega_i)$, where $K^*(j\omega_i)$ is point on the ellipse which is the farthest from the coordinates origin, and $y_*(j\omega_i)$ is the point on the corresponding ellipse that is the closest to the coordinates origin. This prevents from the situation when there is zero value in denominator. So, the problem stops being incorrect, but numerator $y_*(j\omega_i)$ of the ratio $\tilde{x}(j\omega_i)$ sustains a step to zero value at some frequency. This causes Gibbs phenomenon when we perform inverse Fourier transform of $\tilde{x}(j\omega)$. In each concrete case, manual

adjustment of input data error characteristics may decrease effect's influence.

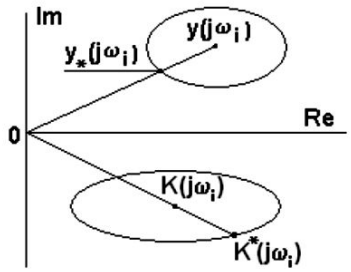

Fig. 1. Illustration of minimal modulus principle

From Fig. 1, it is clear that this solution indeed minimizes the modulus $|x(j\omega)|$, and the condition $\|\mathbf{A}\tilde{x}(t) - y(t)\|^2 = \Delta^2$ holds. After applying the inverse Fourier transform to the solution $\tilde{x}(j\omega_i)$, we get the desired regularized solution to the inverse problem – in other words, we achieve the desired reduction to the ideal measuring instrument. We have shown that this method works very well in many practical situations [10, 11]. This method also allows us to take into account the "objective" prior information about errors and also "subjective" information – as described by (possibly imprecise) expert estimates [6].

2.2. *The inverse filter*

The principle of minimal modulus can only be used after the whole signal is measured. This is reasonable in spectroscopy and chromatography, but in processing dynamic signals, we often need to produce results in real time, before all the measurements are finished. This can be achieved by using an inverse filter, which can be physically implemented as one or several sequential dynamically stable circuits. An example is given on Fig. 2.

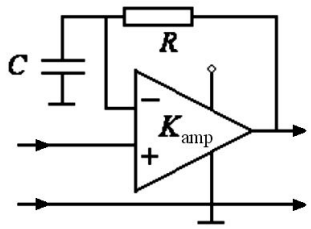

Fig. 2. Inverse filter circuit

If the amplifier gain is K_{amp} and R and C are the resistance and capacitance of inertial RC-circuit, then the complex frequency characteristic (CFC) of circuit on Fig. 2 is equal to

$$K_f(j\omega) = \frac{K_{\text{amp}}}{1+K_{\text{amp}}} \cdot (1 + j\omega RC) \cdot \left[1 + j\omega \cdot \frac{RC}{1+K_{\text{amp}}}\right]^{-1}.$$

This filter can be used if the modulus of CFC of the measuring instrument is monotonically decreasing. For example, such property is usual for thermistors, thermocouples, Hall sensors for current strength etc. Such gauges have first order CFC:

$$K_g(j\omega) = \frac{K_0}{1 + j\omega\tau_g},$$

where τ_g is its time constant and K_0 is gain coefficient for static mode. In this case, if values of R and C for inverse filter (Fig. 2) are such that $RC = \tau_g$, then series of the gauge and the inverse filter placed after it will have CFC equal to

$$K_g(j\omega) \cdot K_f(j\omega) = \frac{K_0 \cdot K_{\text{amp}}}{1+K_{\text{amp}}} \cdot \left[1 + j\omega \cdot \frac{RC}{1+K_{\text{amp}}}\right]^{-1}.$$

We can see that time constant of such series is decreased in $(1+K_{\text{amp}}) >> 1$ times versus τ_g. This causes corresponded response acceleration with the same ratio and represents the solution for inverse problem of signal restoration.

If the order of CFC for the measurement device is larger than one, then the quantity of first-order inverse filters (Fig. 2) that should be concatenated one after another is the same as the order value. The positive result can be achieved with individual tuning of gain and parameters R and C for every first-order circuit. The inverse problem solution can be achieved using the similar inverse filters even for converters whose CFC order cannot be rated.

Let us examine the example of using such inverse filter for ΣΔ – Analog-to-Digital Conversion: let us consider approximation of frequency characteristic for ADC ADS1256 [12]. This ADC is used for digitizing analog signals with frequency bands (0÷25), (0÷50) and (0÷500) Hz. To construct inverse filter to

improve its metrological properties, we should use fractionally rational approximation to ADC frequency characteristics.

To approximate ADS1256 CFC $K_{\text{ADC}}(j\omega)$, we can use separate values of its squared amplitude frequency characteristic (AFC) $\left|K_{\text{ADC}}(j\omega)\right|^2$ that is presented by ADC producer [12]:

$$\left|K_{\text{ADC}}(j\overline{\omega})\right| = \left|\frac{\sin(\pi\cdot\overline{\omega})}{64\cdot\sin(\pi\cdot\overline{\omega}/64)}\right|^5 \cdot \left|\frac{\sin(\pi\cdot\overline{\omega}\cdot N)}{N\cdot\sin(\pi\cdot\overline{\omega})}\right|,$$

where $\overline{\omega} = \omega/\omega_S = f/f_S$ is relative frequency, f is ADC input signal frequency, f_S = 30 kHz is ADC maximum sampling frequency, N is quantity of averaging output values, $\omega = 2\pi f$ and $\omega_S = 2\pi f_S$ are angular frequencies.

The mentioned data points are placed in the second row of table 1. Fractionally rational approximation was performed for function $\left|K_{\text{ADC}}(j\omega)\right|^2$. This function is real-valued, its argument is ω^2. So, we can apply traditional approximation techniques that are developed for real-valued functions.

Two variants of approximation were considered: the case when $N = 1$ and frequency band for approximation is [0, 0.06666] for $\overline{\omega}$ or [0, 2000] Hz for f and the case when $N = 8$ and band is [0, 0.06] for $\overline{\omega}$ or [0, 1800] Hz for f. We use uniform meshes of 81 points for both of cases $N = 1$ and $N = 8$.

The obtained approximations were factorized to get expression for CFC $K_{\text{ADC}}(j\omega)$. The used factorization method is described in [13]. Approximation accuracy was set to 0.3%. As a result, the following CFC were obtained:

$$N = 1: \quad \widetilde{K}_{\text{ADC}}(j\overline{\omega}) = \frac{1}{1 + 4.112\cdot j\overline{\omega}},$$

$$N = 8: \quad \widetilde{K}_{\text{ADC}}(j\overline{\omega}) = \frac{1}{1 + 2\cdot 0.8598\cdot 14.73\cdot j\overline{\omega} - (14.73\cdot\overline{\omega})^2}.$$

In table 1 placed below, values of real AFC $\left|K_{\text{ADC}}(jf)\right|$ and its obtained approximation $\left|\widetilde{K}_{\text{ADC}}(jf)\right|$ are presented for $N = 1$. Fig. 3 illustrates data presented in Table 1. Averaging, that takes a place during analog-to-digital conversation, causes this effect of AFC decreasing.

Table 1. Results of approximation of $K_{\text{ADC}}(jf)$ for ADC ADS1256 ($N = 1$)

f, Hz	0.0	50	100	200	300	400	500	1000	2000
$\lvert K_{\text{ADC}}(jf)\rvert$	1.0	0.99998	0.999909	0.99964	0.99918	0.99854	0.9977	0.9909	0.9641
$\lvert \widetilde{K}_{\text{ADC}}(jf)\rvert$	1.0	0.99998	0.999906	0.99962	0.99916	0.99850	0.9977	0.9907	0.9644

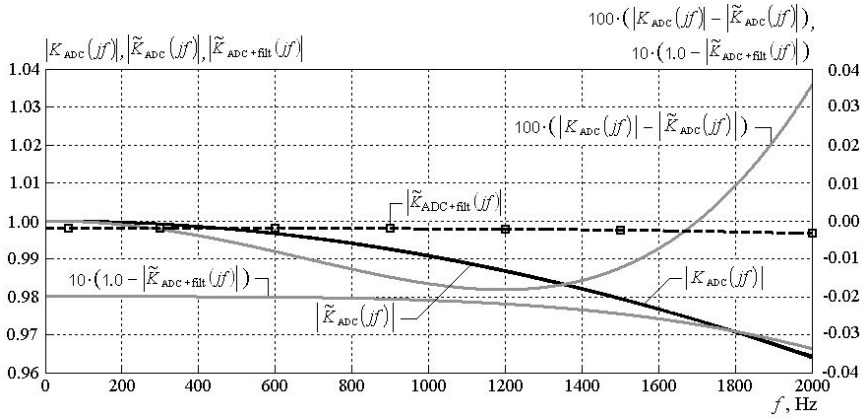

Fig. 3. Results of AFC approximation and correction for ADC ADS1256 (case $N = 1$)

On Fig. 3, a curve for approximation error $|K_{\text{ADC}}(jf)| - |\widetilde{K}_{\text{ADC}}(jf)|$ is also presented. Its scale is put on the right side of the graph.

In Table 2 the results are placed for the case $N = 8$. Fig. 4 contains graphical representation of data from this table.

Table 2. Results of approximation of $K_{\text{ADC}}(jf)$ for ADC ADS1256 ($N = 8$)

f, Hz	0.0	60	300	600	900	1200	1500	1800
$\lvert K_{\text{ADC}}(jf)\rvert$	1.0	0.9996	0.9889	0.9559	0.9025	0.8311	0.7444	0.6463
$\lvert \widetilde{K}_{\text{ADC}}(jf)\rvert$	1.0	0.9996	0.9895	0.9576	0.9035	0.8297	0.7426	0.6513

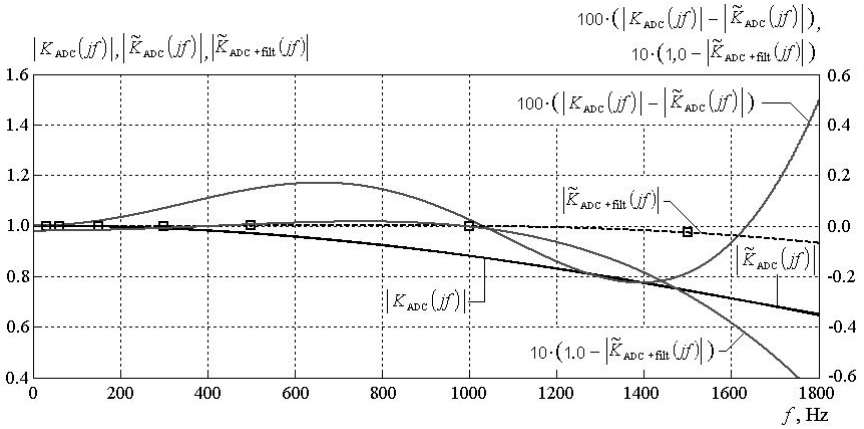

Fig. 4. Results of AFC approximation and correction for ADC ADS1256 (case $N = 8$)

We can see that for frequencies f less than 100 Hz the AFC is close to unit value (difference is less than 0.02%) for both of approximations that is acceptable. For frequencies from 500 to 1000 Hz, the AFC differs from 1.0 with error less than 0.5%. The approximate order of CFC is now determined. Further, our purpose is to construct physically realizable inverse filter that will describe obtained approximation.

Let us take into consideration case $N = 1$.

The CFC approximation has the first order. So, we can use the simplest inverse filter as presented on Fig. 2. Good AFC correction will be obtained if we choose amplifier's gain equal to $K_{\text{amp}} = 500$ and time constant for filter in feedback circuit equal to $\tau_f = R \cdot C$ =21.5 μs. Let $\left|\tilde{K}_{\text{filt}}(jf)\right|$ be AFC of inverse filter. Then, the AFC of inverse filter (first circuit in sequence) and ADC (second circuit in sequence) connection will be $\left|\tilde{K}_{\text{ADC+filt}}(jf)\right| = \left|\tilde{K}_{\text{filt}}(jf)\right| \cdot \left|K_{\text{ADC}}(jf)\right|$.

Values of corrected AFC for some frequencies are presented in Table 3 and put on Fig. 3 (marked as squares and dashed curve) with the values of correction inaccuracy, equal to $1.0 - \left|\tilde{K}_{\text{ADC+filt}}(jf)\right|$ (its scale is on the right side of graph).

Table 3. Correction with the inverse filter for ADC ADS1256 ($N = 1$)

f, Hz	0	60	300	600	900	1200	1500	2000
$\left\|K_{\text{ADC}}(jf)\right\|$	1.00000	0.99997	0.9992	0.9967	0.9926	0.9869	0.9796	0.9641
$\left\|\tilde{K}_{\text{ADC+filt}}(jf)\right\|$	0.99800	0.99804	0.9980	0.9980	0.9979	0.9978	0.9976	0.9966

We see that corrected AFC has essentially wider frequency band.

Let us now take into consideration case $N = 8$.

The simplest realization of inverse filter for correction of second-order CFC that is used to describe ADC time-frequency characteristics is concatenation of two inverse filters of first order. Time constant τ_f for each of them should be about $\tau_f = (1.0 \div 5.0)/f_s$ for $\widetilde{K}_1(\overline{\omega})$ and $\widetilde{K}_2(\overline{\omega})$. Block-scheme of such complex inverse filter is presented on Fig. 5.

Filter of such structure can be easily realized in analog or in digital form. But to obtain higher accuracy, it is better to put inverse filter before ADC and combine it with input gain amplifier.

Time constant τ_f for each of first-order inverse filter on the Fig. 5 should be adjusted using filter mathematical model. It can happen that the best result will be when time constants will be different for these filters. Mathematical modeling can help to determine the best gain value K_{amp} for direct circuits on Fig. 5. They should have work frequency band wider than frequency diapason that is chosen for CFC correction.

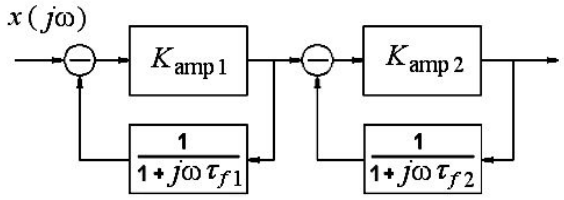

Fig. 5. Block-scheme for inverse filter of second order

Mathematical modeling shows that for case $N = 8$ the satisfactory correction can be achieved if we use two inverse filter of first order, which parameters are $K_{\text{amp 1}} = 1000$, $\tau_{f\,1} = 60$ μs and $K_{\text{amp 2}} = 1000$, $\tau_{f\,2} = 58$ μs. Results of such correction are presented in Table 4 and put on Fig. 4 (marked as squares and dashed curve).

Table 4. Correction with the inverse filter for ADC ADS1256 ($N = 8$)

f, Hz	0	30	60	150	300	500	1000	1500	2000
$\lvert K_{\text{ADC}}(jf)\rvert$	1.00000	0.99989	0.99955	0.99721	0.98886	0.9692	0.8806	0.7445	0.5764
$\lvert \widetilde{K}_{\text{ADC+filt}}(jf)\rvert$	0.99800	0.99802	0.99805	0.99829	0.99909	1.0005	0.9996	0.9728	0.8915

It is clear, that the AFC unevenness for frequency band [0, 1] kHz is less than 0.2%. We can conclude that described technique of inverse filter design allows obtaining measuring channel with wider frequency band and faster response. Such technique can be applied to any measurement instrument or converter with monotonically decreased amplitude frequency characteristics.

References

1. G. Solopchenko, *Measurement Techniques*. **17** (1974).
2. V. Knorring and G. Solopchenko, *Measurement Techniques*. **46**, 546 (2003).
3. G. Vasilenko, *Theoriya vosstanovleniya signalov*. (1979). In Russian.
4. S. Mikhlin, *Mathematical physics: an advanced course*. (1970).
5. A. Tikhonov and V. Arsenin, *Solutions of Ill-Posed Problems*. (1977).
6. V. Kreinovich, C.-C. Chang, L. Reznik and G. Solopchenko, *NASA Conference Publication* (NAFIPS-92), **2**, 418. (1992).
7. G. Solopchenko. *Measurement Techniques*, **44**, 546 (2001).
8. N. Seregina and G. Solopchenko, *Izvestiya AN SSSR*. *Technical cybernetics*, **2**, 166 (1984). In Russian.
9. K. Semenov and G. Solopchenko. *Measurement Techniques*. **53**, 592 (2010).
10. K. Savkov, N. Seregina and G. Solopchenko. *Journal of Advanced Materials*, **1** (2), 205 (1994).
11. N. Seregina, G. Solopchenko. *Pribory i sistemy upravleniya.* (4), 19 (1992) In Russian.
12. ADS1255, ADS1256: Very Low Noise, 24-bit Analog-to-Digital Converter. Texas Instruments technical document SBAS288K. Available at: www.ti.com/lit/ds/sbas288k/sbas288k.pdf.
13. V. Kreinovich, G. Solopchenko. *Measurement Techniques*. **36** (9), 968 (1993).